1976-11

The polar problem in a global prediction model

Williams, R. T.

Monterey, California. Naval Postgraduate School

NPS-63Wu76111

NAVAL POSTGRADUATE SCHOOL
Monterey, California

THE POLAR PROBLEM IN A GLOBAL PREDICTION MODEL

R. T. Williams

November 1976

Technical Report Period January 1976-October 1976

Approved for public release; distribution unlimited.

Prepared for: Naval Environmental Prediction Research Facility, Monterey, CA

NAVAL POSTGRADUATE SCHOOL
Monterey, California

Rear Admiral Isham W. Linder
Superintendent

Jack R. Borsting
Provost

ABSTRACT

This report investigates the behavior of the model developed by Monaco and Williams when the initial flow is over the pole. The numerical solution eventually becomes unstable with this initial state. The difficulty is controlled by modifying the v field on the latitude circle which is closest to the pole.

Released by:

UNCLASSIFIED

SECURITY CLASSIFICATION OF THIS PAGE *(When Data Entered)*

REPORT DOCUMENTATION PAGE		READ INSTRUCTIONS BEFORE COMPLETING FORM
1. REPORT NUMBER NPS-63Wu76111	2. GOVT ACCESSION NO.	3. RECIPIENT'S CATALOG NUMBER
4. TITLE *(and Subtitle)* THE POLAR PROBLEM IN A GLOBAL PREDICTION MODEL		5. TYPE OF REPORT & PERIOD COVERED Technical Report January 1976-October 1976
		6. PERFORMING ORG. REPORT NUMBER
7. AUTHOR(s) R. T. Williams		8. CONTRACT OR GRANT NUMBER(s)
9. PERFORMING ORGANIZATION NAME AND ADDRESS Naval Postgraduate School Monterey, California 93940		10. PROGRAM ELEMENT, PROJECT, TASK AREA & WORK UNIT NUMBERS N6685676WR00008
11. CONTROLLING OFFICE NAME AND ADDRESS Naval Postgraduate School Monterey, California 93940		12. REPORT DATE November 1976
		13. NUMBER OF PAGES 29
14. MONITORING AGENCY NAME & ADDRESS*(if different from Controlling Office)*		15. SECURITY CLASS. *(of this report)* Unclassified
		15a. DECLASSIFICATION/DOWNGRADING SCHEDULE

16. DISTRIBUTION STATEMENT *(of this Report)*

Approved for public release; distribution unlimited.

17. DISTRIBUTION STATEMENT *(of the abstract entered in Block 20, if different from Report)*

18. SUPPLEMENTARY NOTES

19. KEY WORDS *(Continue on reverse side if necessary and identify by block number)*

Finite Difference Equations
Polar Problem

20. ABSTRACT *(Continue on reverse side if necessary and identify by block number)*

This report investigates the behavior of the model developed by Monaco and Williams when the initial flow is over the pole. The numerical solution eventually becomes unstable with this initial state. The difficulty is controlled by modifying the v field on the latitude circle which is closest to the pole.

DD FORM 1 JAN 73 1473 EDITION OF 1 NOV 65 IS OBSOLETE
S/N 0102-014-6601 |

UNCLASSIFIED

SECURITY CLASSIFICATION OF THIS PAGE *(When Data Entered)*

TABLE OF CONTENTS

LIST OF SYMBOLS AND ABBREVIATIONS

A	Arbitrary constant in the stream function
a	Earth's radius
F	Zonal flux term
g^u	Flux term in ξ-equation of motion
g^v	Flux term in η-equation of motion
G	Meridional flux term
I	Number of points around latitude circle
i	Grid index in the ξ-direction
j	Grid index in the η-direction
k	Vertical grid index
m	$1/(a \cos \phi)$
mb	Millibars
NACA	National Advisory Committee on Aeronautics
n	$1/a$
P	Pole on the ij index system
$\dot{S}$	Area-pressure weighted vertical velocity
t	Time
u	Zonal wind
v	Meridional wind
η	Meridional coordinate of the curvilinear coordinate system
$\Delta\eta$	Distance increment in the meridional direction
λ	Longitude
ξ	Zonal coordinate of the curvilinear coordinate system
$\Delta\xi$	Distance increment in zonal direction

π Terrain pressure

Π Area-weighted terrain pressure

σ Dimensionless vertical coordinate

$\Delta\sigma$ Vertical increment in the sigma coordinate system

$\dot{\sigma}$ Measure of vertical velocity

ϕ Latitude

Ω Angular velocity of the earth

I. INTRODUCTION

Most global primitive equation models now in use employ spherical coordinates (see Haltiner and Williams [1975]). Flow crossing the pole presents a potential problem in this coordinate system. Mihok and Kaitala (1976) have described a global prediction model which is in the last stages of development at the Fleet Numerical Prediction Central. McCollough (1974) in testing an earlier version of this model observed the development of large gradients in the surface pressure near the pole when a particular real data set was used. Maher (1974) examined this problem more closely by using analytic initial data which gave a strong flow across the pole. His solutions showed that the pressure field was spuriously disturbed by the finite differencing near the pole. He was able to reduce the effect by various types of smoothing.

In this report we will test a somewhat different finite difference scheme and we will test a procedure for controlling the problem. The Navy Environmental Prediction Research Facility is now testing the global prediction model which was developed by Arakawa and Mintz (1974). In this study we will employ the model which was described by Monaco and Williams (1975). This model is a slightly simplified version of the Arakawa model and it differs from the FNWC model mainly with respect to the spatial staggering of the variables.

II. FINITE DIFFERENCE EQUATIONS

The basic differential and difference equations used in this study are given in Monaco and Williams (1975).[1] Here we will reproduce only those difference equations which have been changed. Fig. 1 shows the arrangement of variables in the model. The list of symbols gives the various definitions. The finite difference continuity equation has the following form:

$$\frac{\partial \tilde{\pi}_{i,j}}{\partial t} + F^k_{i+\frac{1}{2},j} - F^k_{i-\frac{1}{2},j} + G^k_{i,j+\frac{1}{2}} - G^k_{i,j-\frac{1}{2}}$$

$$+ \frac{1}{\Delta\sigma^k}(\dot{S}^{k+1}_{i,j} - \dot{S}^{k-1}_{i,j}) = 0. \tag{2.1}$$

The mass fluxes are defined

$$F^k_{i+\frac{1}{2},j} = \overline{\tfrac{1}{2}(u\tfrac{\Delta\eta}{n})}^{k}_{i+\frac{1}{2},j}(\pi_{i+i,j} + \pi_{i,j}), \tag{2.2}$$

$$G^k_{i,j+\frac{1}{2}} = \tfrac{1}{2}(v\tfrac{\Delta\xi}{m})^k_{i,j+\frac{1}{2}}(\pi_{i,j+1} + \pi_{i,j}), \tag{2.3}$$

where

$$\tilde{\pi}_{i,j} \equiv \pi_{i,j}\left(\frac{\Delta\xi\Delta\eta}{mn}\right)_{i,j},$$

$$\dot{S}_{i,j} \equiv \tilde{\pi}_{i,j}\dot{\sigma}_{i,j} \quad .$$

The bar in (2.2) represents zonal smoothing as described in MW.

---

[1] Hereafter we will refer to this reference as MW.

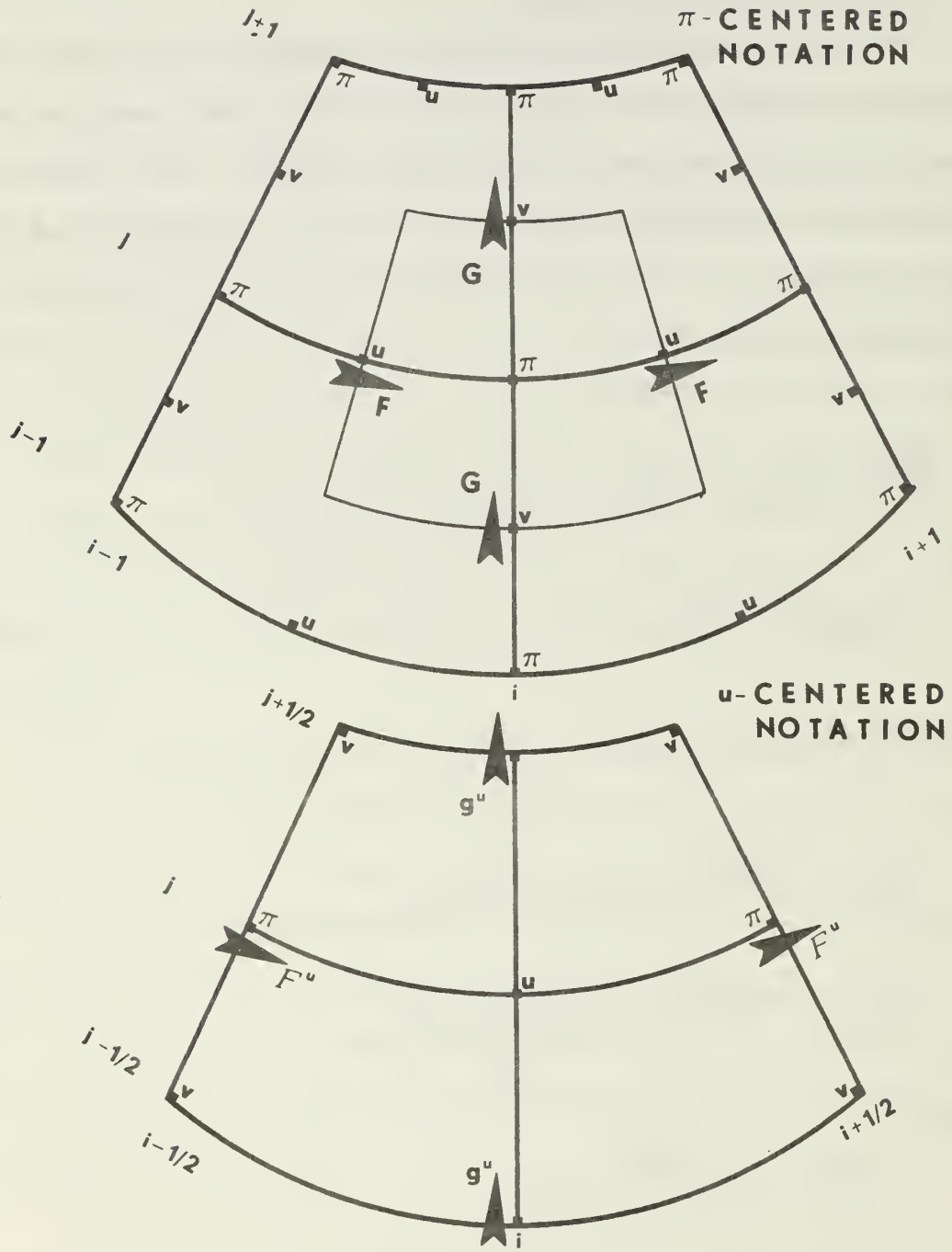

Figure 1. An example of the notation used to describe the finite difference equations. The continuity equation is described on a "π-centered" grid in which the F and G symbols are flux calculations in their respective directions. The "u-centered" grid is an example used to describe the ξ-component of the equation of motion where F^u and g^u are also flux calculations.

The left hand side of the zonal momentum equation is:

$$\frac{\partial}{\partial t}(\overline{\Pi}^{u}_{i,j} u^{k}_{i,j}) + \tfrac{1}{2}[F^{u}_{i+\frac{1}{2},j}(u_{i+1,j} + u_{i,j})^{k}$$

$$- F^{u}_{i-\frac{1}{2},j}(u_{i,j} + u_{i-1,j})^{k} + g^{u}_{i,j+\frac{1}{2}}(u_{i,j+1} + u_{i,j})^{k} - g^{u}_{i,j-\frac{1}{2}}(u_{i,j} + u_{i,j-1})^{k}]$$

$$+ \frac{1}{\Delta\sigma^{k}} \tfrac{1}{2}[\dot{S}^{u,k+1}_{i,j}(u^{k+2}_{i,j} + u^{k}_{i,j}) - \dot{S}^{u,k-1}_{i,j}(u^{k}_{i,j} + u^{k-2}_{i,j})] \qquad (2.4)$$

where

$$\overline{\Pi}^{u}_{i,j} \equiv \frac{1}{8}[\overline{\Pi}_{i+\frac{1}{2},j+1} + \overline{\Pi}_{i-\frac{1}{2},j+1} + \overline{\Pi}_{i-\frac{1}{2},j-1} + \overline{\Pi}_{i+\frac{1}{2},j-1} + 2(\overline{\Pi}_{i+\frac{1}{2},j} + \overline{\Pi}_{i-\frac{1}{2},j})], \qquad (2.5)$$

$$\dot{S}^{u}_{i,j} \equiv \frac{1}{8}[\dot{S}_{i+\frac{1}{2},j+1} + \dot{S}_{i-\frac{1}{2},j+1} + \dot{S}_{i-\frac{1}{2},j-1} + \dot{S}_{i+\frac{1}{2},j-1} + 2(\dot{S}_{i+\frac{1}{2},j} + \dot{S}_{i-\frac{1}{2},j})]. \qquad (2.6)$$

The above definitions (2.5) and (2.6) are more complicated than those in MW and they are the same as those used by Arakawa and Mintz (1974). The quantities F^{u} and g^{u} are defined as follows:

$$F^{u}_{i+\frac{1}{2},j} \equiv \frac{1}{4}(F^{*}_{i+\frac{1}{2},j+1} + 2F^{*}_{i+\frac{1}{2},j} + F^{*}_{i+\frac{1}{2},j-1}), \qquad (2.7)$$

$$g^{u}_{i,j+\frac{1}{2}} \equiv \frac{1}{4}(G^{*}_{i+\frac{1}{2},j} + G^{*}_{i+\frac{1}{2},j+1} + G^{*}_{i-\frac{1}{2},j} + G^{*}_{i-\frac{1}{2},j+1}), \qquad (2.8)$$

where

$$F^{*}_{i,j} \equiv \tfrac{1}{2}(F_{i+\frac{1}{2},j} + F_{i-\frac{1}{2},j}), \qquad (2.9)$$

$$G^{*}_{i,j} \equiv \tfrac{1}{2}(G_{i,j+\frac{1}{2}} + G_{i,j-\frac{1}{2}}). \qquad (2.10)$$

The left hand side of the meridional momentum equation takes the same form as (2.4) when u is replaced by v. The other quantities are defined as follows:

$$F^{v}_{i+\frac{1}{2},j} \equiv \frac{1}{4}(F^{*}_{i+1,j+\frac{1}{2}} + F^{*}_{i,j+\frac{1}{2}} + F^{*}_{i,j-\frac{1}{2}} + F^{*}_{i+1,j-\frac{1}{2}}), \tag{2.11}$$

$$g^{v}_{i,j+\frac{1}{2}} \equiv \frac{1}{4}(G^{*}_{i+1,j+\frac{1}{2}} + 2G^{*}_{i,j+\frac{1}{2}} + G^{*}_{i-1,j+\frac{1}{2}}), \tag{2.12}$$

$$\Pi^{v}_{i,j} \equiv \frac{1}{8}[\Pi_{i+i,j+\frac{1}{2}} + \Pi_{i-1,j+\frac{1}{2}} + \Pi_{i-1,j-\frac{1}{2}} + \Pi_{i+i,j-\frac{1}{2}} + 2(\Pi_{i,j+\frac{1}{2}} + \Pi_{i,j-\frac{1}{2}})], \tag{2.13}$$

$$\dot{S}^{v}_{i,j} \equiv \frac{1}{8}[\dot{S}_{i+1,j+\frac{1}{2}} + \dot{S}_{i-1,j+\frac{1}{2}} + \dot{S}_{i-1,j-\frac{1}{2}} + \dot{S}_{i+1,j-\frac{1}{2}} + 2(\dot{S}_{i,j+\frac{1}{2}} + \dot{S}_{i,j-\frac{1}{2}})]. \tag{2.14}$$

The definitions (2.13) and (2.14) are more complicated than those in MW and they are the same as those used by Arakawa.

Arakawa and Mintz (1974) derived the expressions (2.5) and (2.6) for Π and $\dot{S}$ at the u points in the following way. The u field in (2.4) is set equal to a constant. Then the continuity equation (2.1) is averaged from surrounding points in such a way that the average has the same form as (2.4) with u = constant. This is a reasonable requirement and it is necessary for energy conservation. This average gives the expressions (2.5) and (2.6). The definitions (2.13) and (2.14) are derived in the same way by setting v = constant in the appropriate equations.

These difference expressions must be modified near the pole because some of the quantities are not defined at the pole. Fig. 2 shows the points near the pole which are used to evaluate the pressure change at the pole. The pole is composed of I points which are denoted by (i, P).

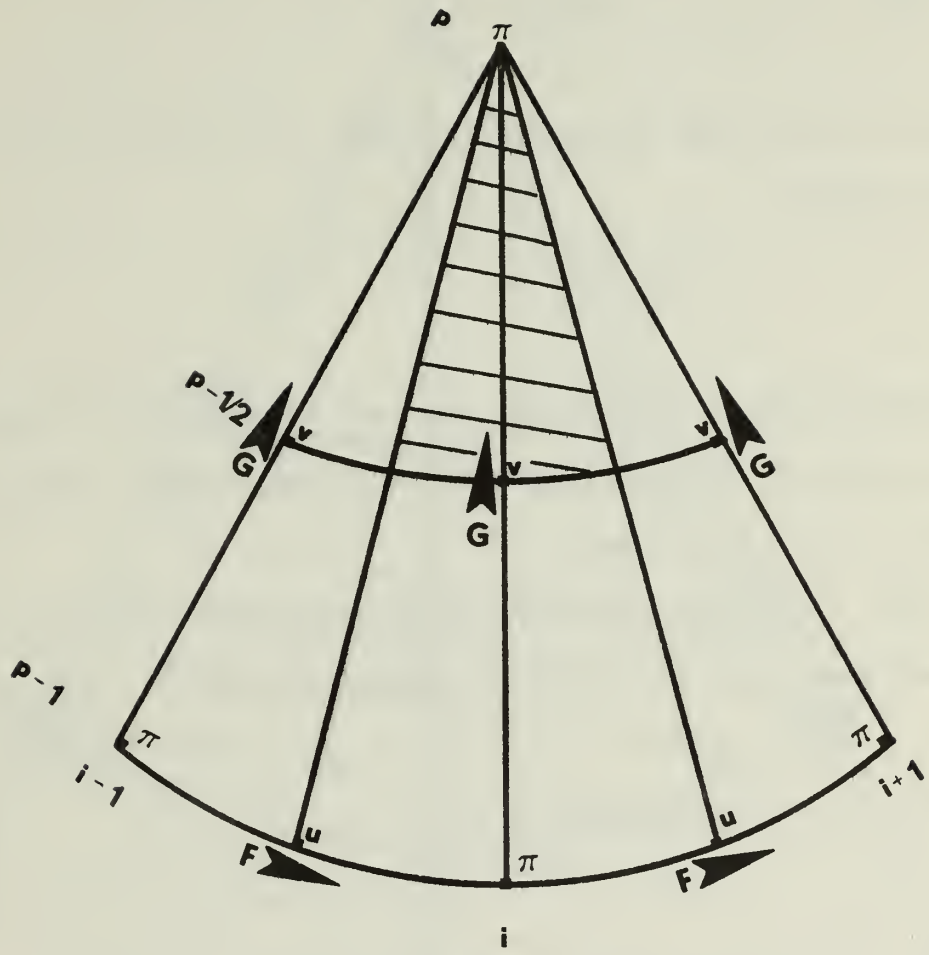

Figure 2. Each index i,P in the continuity equation is represented by the shaded area. π at the poles can only change as a result of G. The thermodynamic equation and vertical velocity are treated in the same manner.

The continuity equation applied at each of these points is written:

$$\frac{\partial \pi_{i,P}}{\partial t} - G^{k}_{i,\,P-\frac{1}{2}} + \frac{1}{\Delta\sigma^{k}}(\dot{S}^{k+1}_{i,P} - \dot{S}^{k-1}_{i,P}) = 0. \qquad (2.15)$$

After each time step the surface pressure at the pole (P) is set equal to the average:

$$P \equiv \frac{1}{I}\sum_{i=1}^{I} \pi_{i,P} \quad . \qquad (2.16)$$

If we sum (2.18) in the vertical and use (2.16) we can see that the pressure at the pole changes in proportion to the net mass flux across the latitude circle at $j = P-\frac{1}{2}$.

Fig. 3 shows the quantities which are needed to predict u at j = P-1. The left hand side of the zonal momentum equation at j = P-1, takes the form:

$$\frac{\partial}{\partial t}(\pi^{u} u^{k})_{i,P-1} + \tfrac{1}{2}[F^{*u}_{i+\frac{1}{2},P-1}(u_{i,P-1} + u_{i+1,P-1})^{k}$$

$$-F^{*u}_{i-\frac{1}{2},P-1}(u_{i,P-1} + u_{i-1,P-1})^{k} - g^{u}_{i,P-3/2}(u_{i,P-1} + u_{i,P-2})^{k}]$$

$$+ \frac{1}{\Delta\sigma^{k}} \tfrac{1}{2}[\dot{S}^{u,k+1}(u^{k+2}_{i,P-1} + u^{k}_{i,P-1}) - \dot{S}^{u,k-1}(u^{k}_{i,P-1} + u^{k-2}_{i,P-2})], \qquad (2.17)$$

where

$$F^{*u}_{i-\frac{1}{2},P-1} \equiv \frac{1}{4}(4F^{*}_{i-\frac{1}{2},P-1} + F^{*}_{i-\frac{1}{2},P-2}) \ , \qquad (2.18)$$

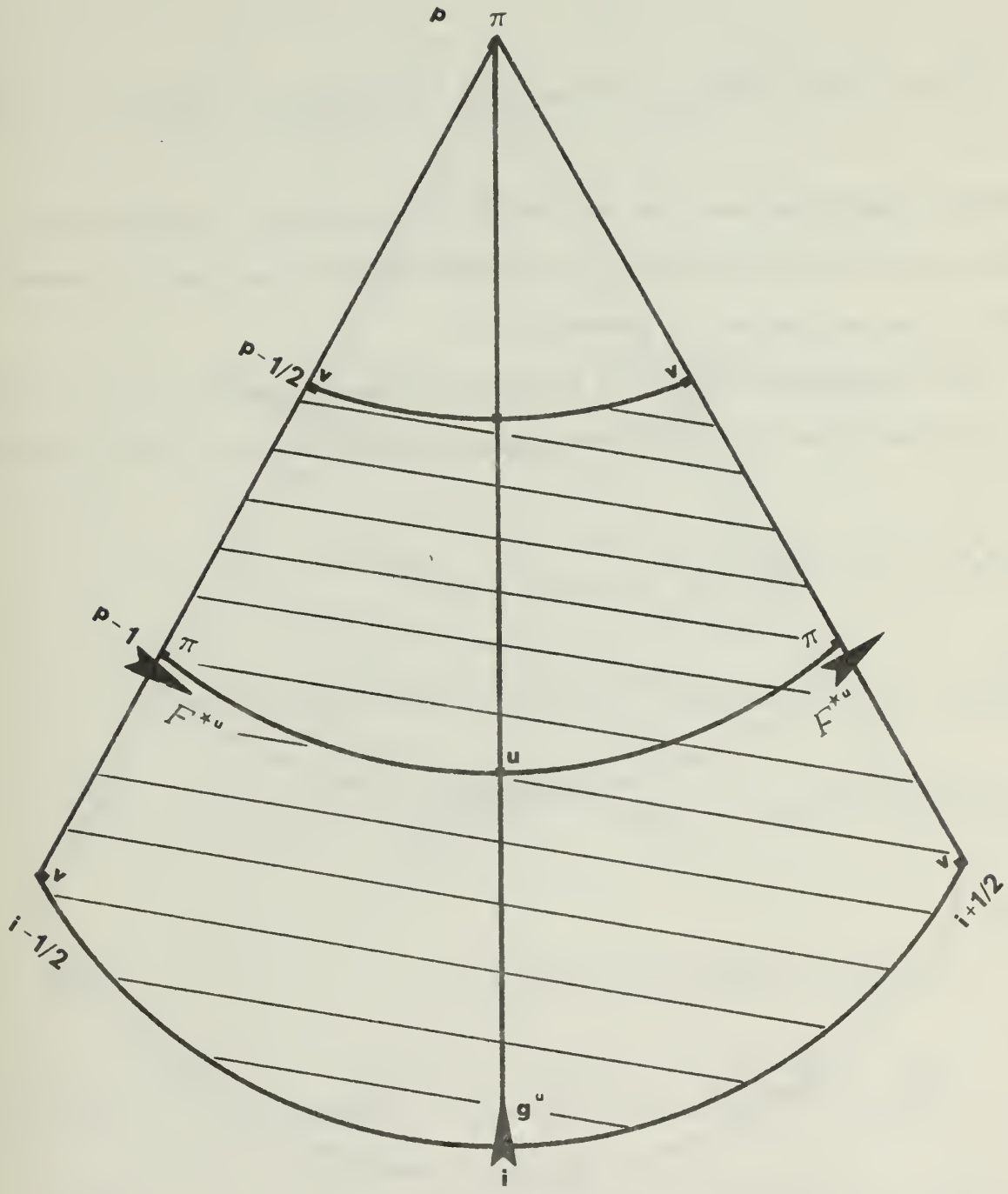

Figure 3. The polar modification of the u equation of motion. F^{*u} and g^u are flux terms. The shaded portion represents the area associated with each variable u.

$$\pi^{u}_{i,P-1} \equiv \pi_P + \frac{3}{8}(\pi_{i-\frac{1}{2},P-1} + \pi_{i+\frac{1}{2},P-1}) + \frac{1}{8}(\pi_{i-\frac{1}{2},P-2} + \pi_{i+\frac{1}{2},P-2}) \quad , \qquad (2.19)$$

$$\dot{S}^{u}_{i,P-1} \equiv \dot{S}_P + \frac{3}{8}(\dot{S}_{i-\frac{1}{2},P-1} + \dot{S}_{i+\frac{1}{2},P-1}) + \frac{1}{8}(\dot{S}_{i-\frac{1}{2},P-2} + \dot{S}_{i+\frac{1}{2},P-2}). \qquad (2.20)$$

The other quantities have the same definitions as above. The relations (2.19) and (2.20) are different from those used by MW and they correspond to the relations derived by Arakawa.

Fig. 4 shows the quantities which are needed to predict v at $j = P-\frac{1}{2}$. The left hand side of the meridional momentum equation at $j = P-\frac{1}{2}$, takes the form:

$$\frac{\partial}{\partial t}(\pi^{v} v^{k})_{i,P-\frac{1}{2}} + \tfrac{1}{2}[F^{*v}_{i+\frac{1}{2},P-\frac{1}{2}}(v_{i+1,P-\frac{1}{2}} + v_{i,P-\frac{1}{2}})^{k}$$

$$-F^{*v}_{i-\frac{1}{2},P-\frac{1}{2}}(v_{i,P-\frac{1}{2}} + v_{i-1,P-\frac{1}{2}})^{k} - g^{v}_{i,P-1}(v_{i,P-\frac{1}{2}} + v_{i,P-3/2})^{k}]$$

$$+ \frac{1}{\Delta\sigma^{k}} \tfrac{1}{2}[\dot{S}^{v,k+1}(v^{k+2}_{i,P-\frac{1}{2}} + v^{k}_{i,P-\frac{1}{2}}) - \dot{S}^{v,k-1}(v^{k}_{i,P-\frac{1}{2}} + v^{k-2}_{i,P-\frac{1}{2}})], \qquad (2.21)$$

where

$$F^{*v}_{i-\frac{1}{2},P-\frac{1}{2}} \equiv \frac{1}{4}(F^{*}_{i-1,P-1} + F^{*}_{i,P-1}), \qquad (2.22)$$

$$\pi^{v}_{i,P-\frac{1}{2}} \equiv \pi_P + \frac{1}{8}(\pi_{i-1,P-1} + \pi_{i+1,P-1} + 2\pi_{i,P-1}), \qquad (2.23)$$

$$\dot{S}^{v}_{i,P-\frac{1}{2}} \equiv \dot{S}_P + \frac{1}{8}(\dot{S}_{i-1,P-1} + \dot{S}_{i+1,P-1} + 2\dot{S}_{i,P-1}) \; . \qquad (2.24)$$

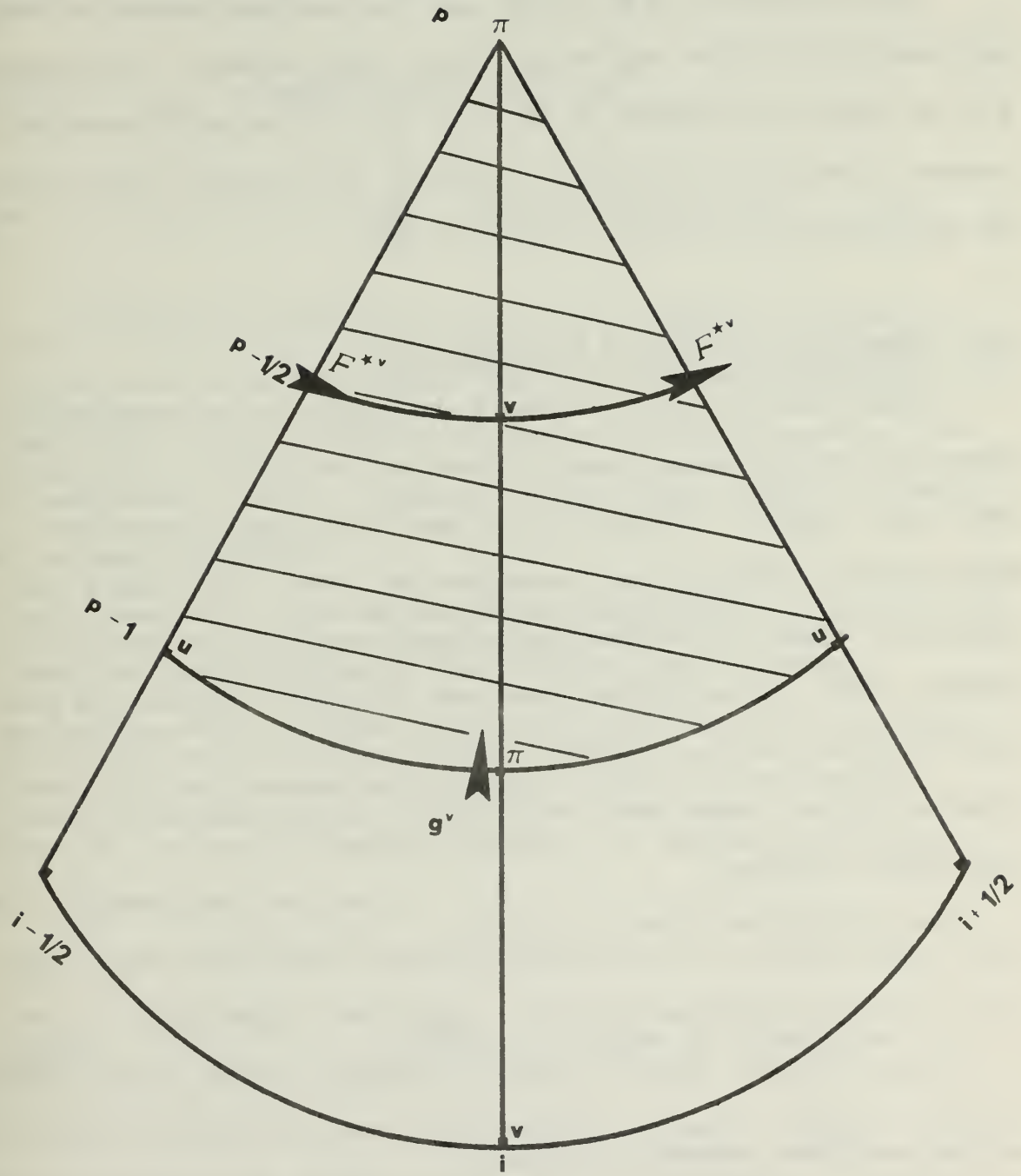

Figure 4. The polar modification of the v equation of motion. F^{*v} and g^{*v} are flux terms. The shaded portion represents the area associated with each variable v.

The relations (2.23) and (2.24) are different from those used by MW and they are equal to the relations derived by Arakawa.

The expressions for Π^u and Π^v near the pole were derived by Arakawa and Mintz (1974) in the same manner as for other latitudes. For example, u is set equal to a constant in Eq.(2.17) and the continuity equation is averaged to achieve the same form. However, the derivation used (2.15), but does not use the average condition (2.16).

III. NUMERICAL SOLUTION WITH FLOW OVER POLE

In this section we will examine a numerical solution which was obtained with the difference equation described in section 2. The initial conditions, which are similar to those used by Holloway, Spelman and Manabe (1973), contain strong flow across the poles. The initial conditions are taken from the barotropic Rossby wave solution developed by Haurwitz (1940). These initial data lead to an exact solution for barotropic horizontal motion (Neamtan [1946]). However, in our model the divergence will not remain zero, but the exact solution should be close to the Haurwitz solution.

The initial zonal wind is given by

$$u(\lambda,\phi,\sigma,0)=-\frac{A}{a}\sin\lambda[\cos^2\phi-\sin^2\phi], \tag{3.1}$$

and the meridional component is given by

$$v(\lambda,\phi,\sigma,0)=\frac{A}{a}\cos\lambda\sin\phi. \tag{3.2}$$

These fields describe wavenumber 1 planetary flow with no mean current. The initial surface pressure is given by

$$\pi(\lambda,\phi,t) = \pi_{ave} + K[(\frac{A}{2a})^2(2\cos^4\phi - \cos^2\phi - 2)$$

$$+ \frac{\Omega A}{3}\cos\phi(5 - 4\cos^2\phi)\sin\lambda + (\frac{A}{2a})^2\cos^2\phi(3 - 2\cos^2\phi)\cos\lambda\,]. \qquad (3.3)$$

Here π_{ave} is the mean surface pressure and K is a constant of proportionality. This solution for the pressure field was obtained by Phillips (1959) and is equivalent to the solution of the nonlinear balance equation. The initial temperature field is a function of height only, and it is given by the NACA standard atmosphere.

Fig. 5 shows the initial surface pressure field in the vicinity of the pole. Note the strong geostrophic flow directly across the pole.

The tests described in this report were carried out with a two-level model, with 45 points between the poles and 10 points in the east-west direction. A time step of 6 minutes was used. No heating, friction or surface topography were included.

Fig. 6 shows the surface pressure prediction of t = 54 hours which was made from the above initial conditions. The basic pattern has rotated considerably from its initial orientation because the wave number 1 initial state excites a Rossby wave which moves rapidly westward. However, in the vicinity of the pole the isobars have become quite distorted. In the non-divergent solution obtained by Neamtan (1946) the initial disturbance rotates at constant angular velocity without distortion. Although in our model the

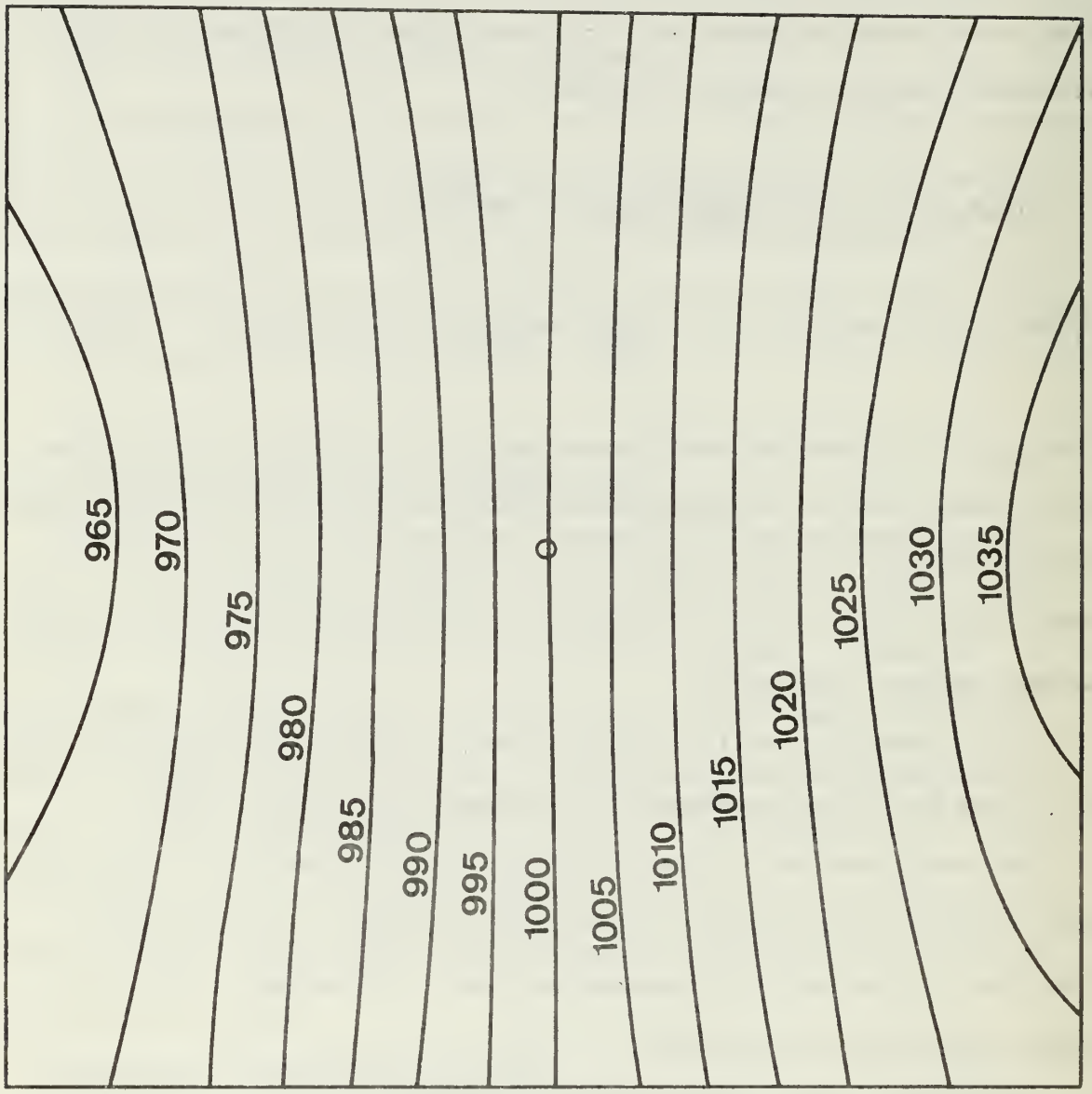

Figure 5. The initial surface pressure field in the vicinity of the pole. The location of the pole is indicated by the small circle in the center.

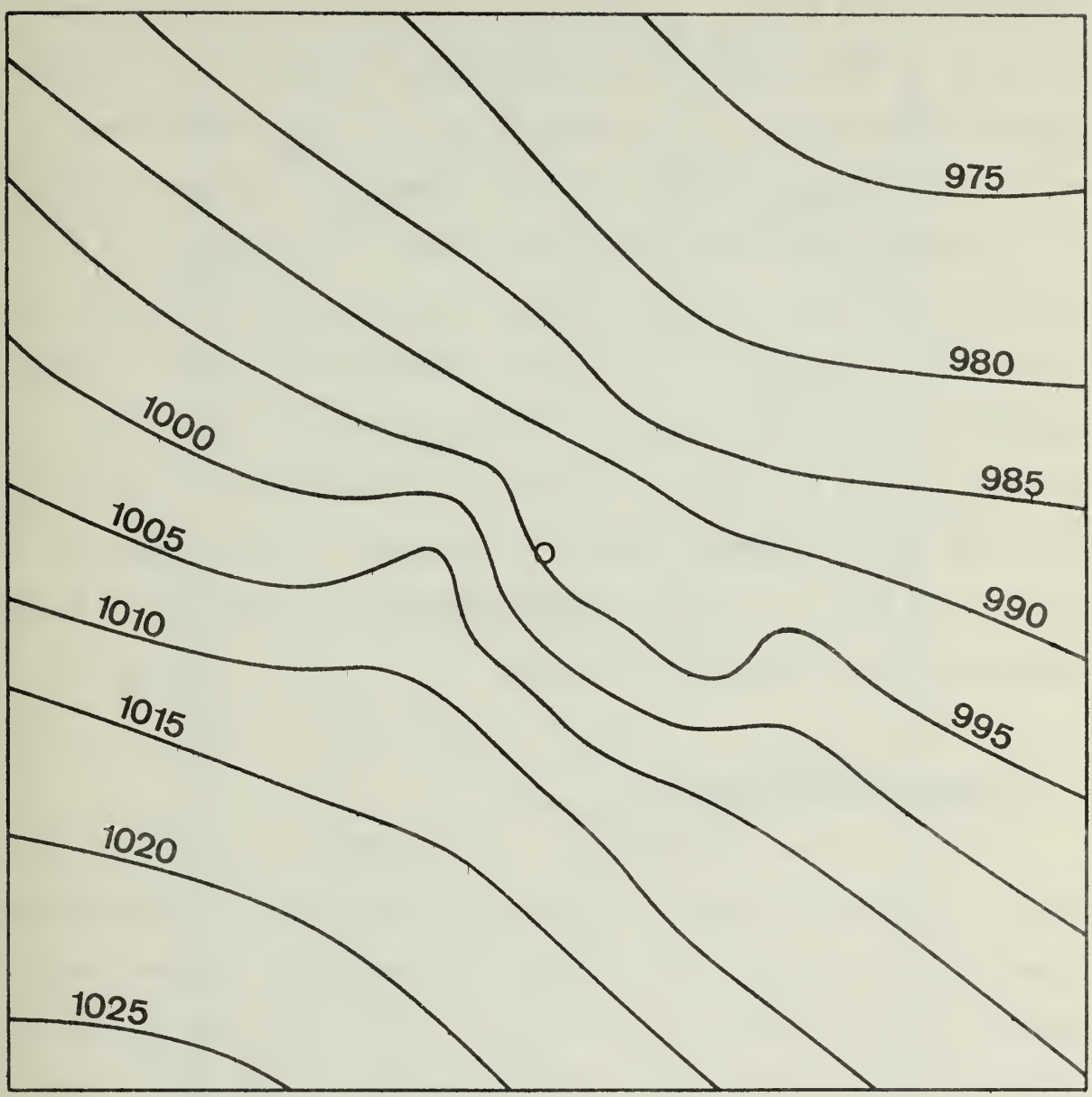

Figure 6. The surface pressure field in the vicinity of the pole at t = 54 hours.

divergence is not zero, it is expected that the general behavior should be similar to the behavior of the nondivergent solutions. Thus the distortions which appear in Fig. 6 near the pole are of a computational nature. In fact, the numerical solution "blew-up" at about t = 75 hours.

In order to consider this problem further, let us examine the V^1 component of the velocity near the pole. In the upper part of Fig. 7 is the initial v component at $\phi = 88^o$; the v component at $\phi = 84^o$ is almost identical. In the lower portion of Fig. 7 are the v^1 fields at the 2 latitudes for t = 54 hours. The fields are somewhat out of phase with each other and the component nearest to the pole is greatly amplified. After t = 54 hours the maximum v component continues to grow until the numerical solution is completely destroyed.

IV. CONTROL OF POLAR PROBLEM

In Fig. 7 it was seen that the v field along the row of points next to the pole becomes very large and irregular as the numerical solution becomes unrealistic. It appears that the geostrophic adjustment process cannot operate effectively along the row of points next to the pole ($\phi = 88^o$ in our experiments). For example, if the v component is too large at one point, then it would modify the polar value of the pressure, which would change the pressure gradient at the original points. However, this process cannot operate freely because the polar pressure changes in proportion to all the points of $\phi = 88^o$, not just one (see Eqs. (2.15) and (2.16)). It is true that various quantities near the pole such as (2.22) and (2.23) and (2.24) were derived by assuming consistency between the momentum change at $\phi = 88^o$ and the pressure changes at surrounding points. But this proof

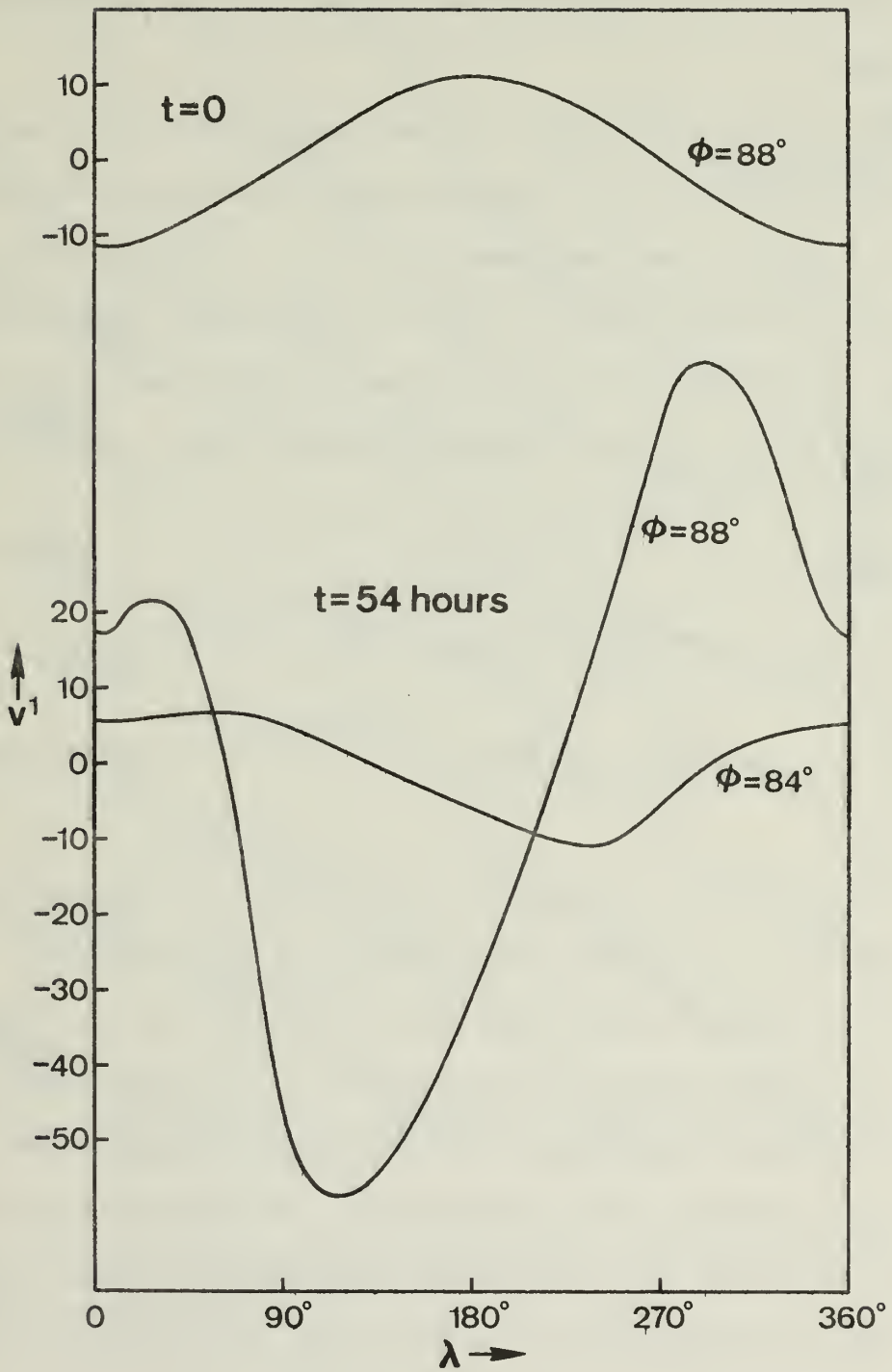

Figure 7. The v^2 field as a function of longitude at t = 0 and t = 54 hours at the latitudes indicated.

is not strictly valid because it assumes different values of $\pi_{i,P}$ (see Eq. (2.15)) for different longitudes whereas (2.16) is enforced at every time step.

In order to avoid this problem it seems appropriate to keep only that portion of the v field at $\phi = 88^{o}$ that can achieve geostrophic balance. This restricts the v field to just wave numbers 0 and 1. With wave number 0 we have the proper interaction with the polar pressure, since v is independent of longitude. The velocity vector is the same on both sides of the pole with wavenumber 1, so that the polar pressure should not change. Thus after every time step we set

$$v_{i,P-\frac{1}{2}} = \frac{1}{I}\sum_{i=1}^{I} v_{i,P-\frac{1}{2}} + \frac{2}{I}\left(\sum_{i=1}^{I} v_{i,P-\frac{1}{2}}\cos\left(\frac{2\pi i}{I}\right)\right)\cos\left(\frac{2\pi i}{I}\right)$$

$$+ \frac{2}{I}\left(\sum_{i=1}^{I} v_{i,P-\frac{1}{2}}\sin\left(\frac{2\pi i}{I}\right)\right)\sin\left(\frac{2\pi i}{I}\right). \qquad (4.1)$$

Fig. 8 shows the surface pressure field at t = 54 hours when (4.1) is used every time step. In this case the isobars are still distorted near the pole, but not nearly as much as in Fig. 6. In Fig. 9 we see the predicted v^{1} fields at the 2 highest latitudes for t = 54 hours. These fields are much closer to the initial fields than those shown in Fig. 7. There is a small increase in the velocity at $\phi = 88^{o}$ and both fields are quite smooth. Of course $v_{i,P-\frac{1}{2}}$ is forced to be smooth by (4.1). Fig. 10 shows the surface pressure field at t = 108 hours. It is actually smoother than at t = 54 hours, although the later solution does have some tilt. It should be noted that the total disturbances amplitude has decreased by about 20% at t = 108 hours. This is apparently due to the Euler-backward restart

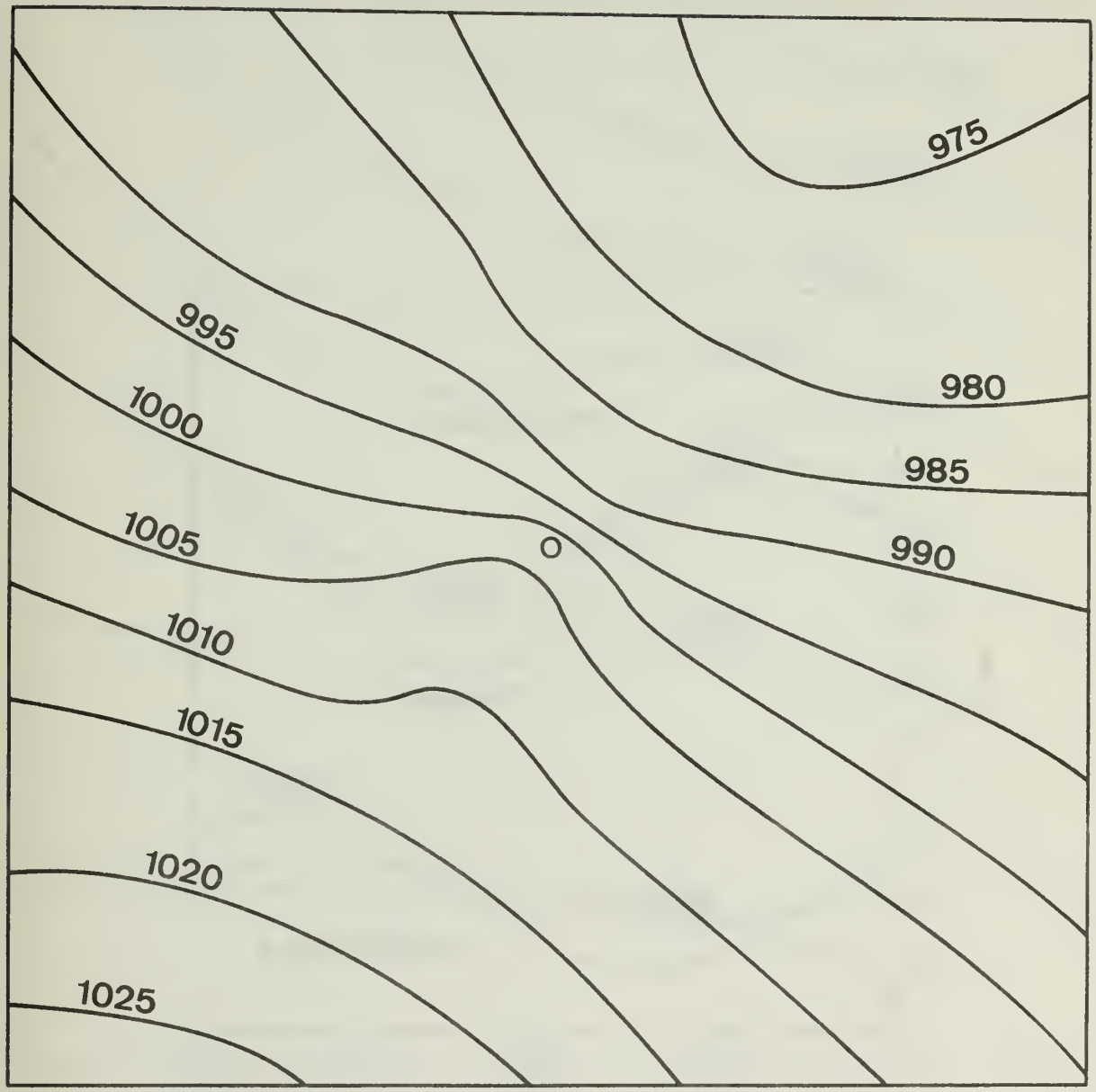

Figure 8. The surface pressure field at t = 54 hours obtained with the modified v structure.

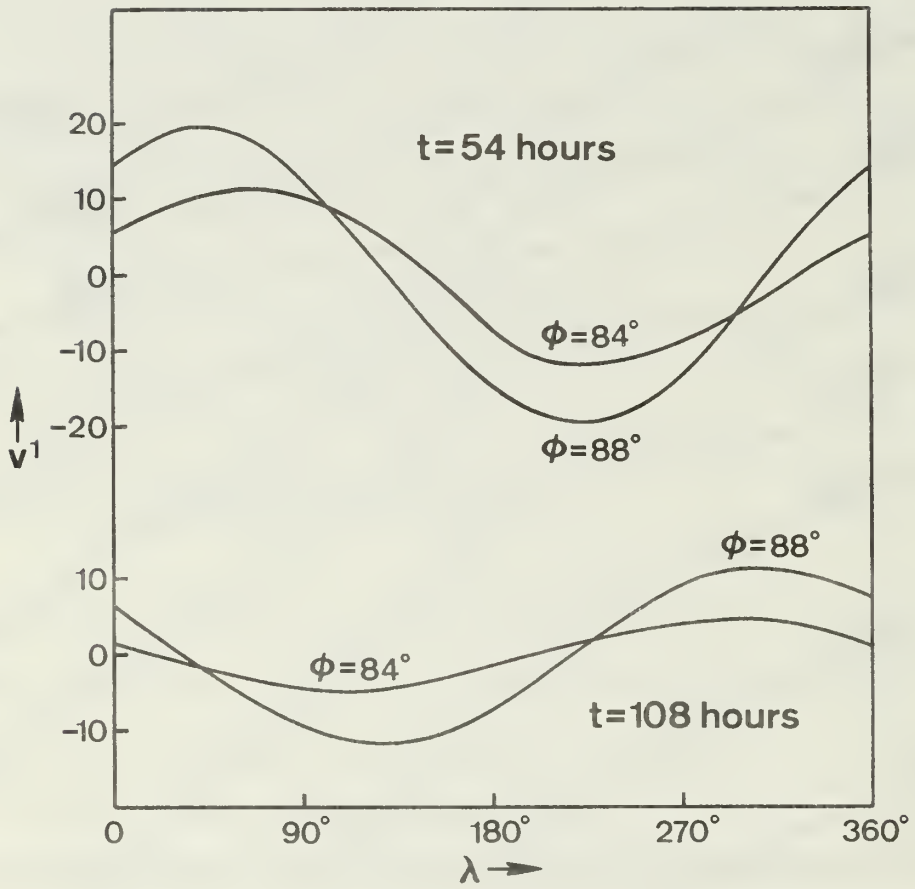

Figure 9. The v^2 field as a function of longitude obtained with the modified v structure for t = 54 hours and t = 108 hours.

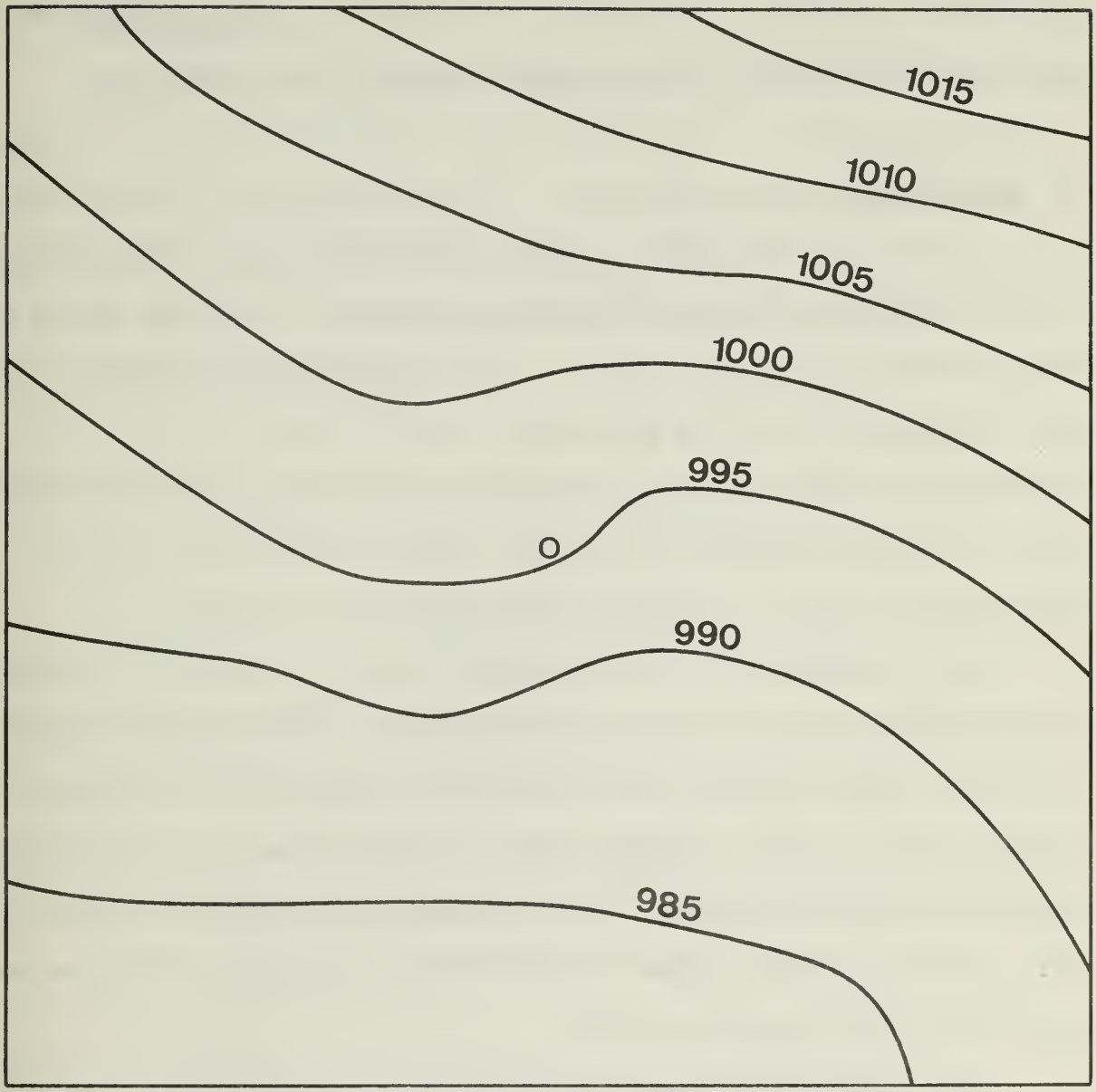

Figure 10. The surface pressure field at t = 108 hours obtained with the modified v structure.

which is used in the model every 30 minutes and to the high frequency of the Rossby wave in this case. The v^1 field near the pole is smooth and has a small amplitude as may be seen in the lower portion of Fig. 9.

V. CONCLUSIONS

It has been shown that the global model developed by Monaco and Williams (1975) is inaccurate when there is flow over the pole, and in fact the model may become unstable. This instability was attributed to the difficulty in achieving geostrophic adjustment near the pole. This is because the polar pressure is changed by the average mass flux across the row of points nearest to the pole. Thus the polar pressure reacts only weakly to the v at a single point adjacent to the pole.

The instability was eliminated when the $v_{i,P-\frac{1}{2}}$ field was replaced by its average plus the first wave in longitude. The resulting integrations were stable and the fields were smooth, although some distortion still occurred near the pole. Sadourny (1975) has formulated a global model in cylindrical coordinates which conserves mean square potential vorticity. His solutions with wave number 1 appear to be quite good, although he does not show the detail near the pole.

The technique developed in this report may be useful for controlling the polar problem in other global models. It could be used in the model described by Mihok and Kaitala (1976) which is now under development at the Fleet Numerical Weather Central. In this application the fields u, v, π and T would all have to be treated since they all occur on the same latitude circle.

VI. ACKNOWLEDGEMENTS

The author wishes to thank Professor G. J. Haltiner for reading the manuscript and making several useful comments on it. The author also benefited from discussions with Dr. D. Dietrick on this problem. The manuscript was typed by Miss M. G. Nichols and the figures were drafted by Mr. M. McDermet. The numerical computations were performed by the W. R. Church Computer Center.

LIST OF REFERENCES

Arakawa, A. and Y. Mintz, 1974 : The UCLA General Circulation Model. Workshop Notes, I-VIII, Department of Meteorology, UCLA.

Haltiner, G. J. and R. T. Williams, 1975 : Some Recent Advances in Numerical Weather Prediction. Monthly Weather Review, 103, 571-590.

Haurwitz, B., 1940 : The Motion of Atmospheric Disturbances on the Spherical Earth. J. Marine Research, 3, 254-267.

Holloway, J. L., M. J. Spelman and S. Manabe, 1973 : Latitude-Longitude Grid Suitable for Numerical Time Integration of a Global Atmospheric Model. Monthly Weather Review, 101, 69-78.

Maher, D. E., 1974: Experiments with a 5-level Global Primitive Equation Atmospheric Model Using Analytically Determined Fields. M.S. Thesis, Naval Postgraduate School, Monterey, California.

McCollough, J. M., 1974: Fourth-order Differencing in a Five-level Spherical Sigma Coordinate Global Weather Prediction Model. M.S. Thesis, Naval Postgraduate School, Monterey, California.

Mihok, W. F. and J. E. Kaitala, 1976: U. S. Navy Fleet Numerical Weather Central Operational Five-level Global Fourth-order Primitive-equation Model. To be published in the Monthly Weather Review.

Monaco, A. V. and R. T. Williams, 1975: An Atmospheric Global Prediction Model Using a Modified Arakawa Differencing Scheme. Naval Postgraduate School Report NPS-51Wu75041.

Neamtan, S. M., 1946 : The Motion of Harmonic Waves in the Atmosphere. J. Meteorology, 3, 53-56.

Phillips, N. A., 1959 : Numerical Integration of the Primitive Equations on the Hemisphere. Monthly Weather Review, 87, 333-345.

Sadourny, R., 1975 : Compressible Model Flows on the Sphere. J. Atmospheric Sciences, 32, 2103-2110.

DISTRIBUTION LIST

		No. Copies
1.	Defense Documentation Center Cameron Station Alexandria, Virginia 22314	2
2.	Library, Code 0212 Naval Postgraduate School Monterey, California 93940	2
3.	Dr. R. T. Williams, Code 63Wu Department of Meteorology Naval Postgraduate School Monterey, California 93940	20
4.	Captain C. R. Ward Director, Naval Oceanography and Meteorology National Space Technology Laboratories Bay St. Louis, Mississippi 39520	1
5.	Captain P. A. Petit Naval Environmental Prediction Research Facility Monterey, California 93940	10
6.	Dean of Research Naval Postgraduate School Monterey, California 93940	2
7.	Captain R. E. Hughes Fleet Numerical Weather Central Naval Postgraduate School Monterey, California 93940	10
8.	Naval Oceanographic Office Library (Code 3330) Washington, D.C. 20373	1
9.	AFCRL - Research Library L. G. Hanscom Field ATTN: Nancy Davis/Stop 29 Bedford, Massachusetts 01730	1
10.	Commander, Air Weather Service Military Airlift Command United States Air Force Scott Air Force Base, Illinois 62226	1

11. Dr. A. Arakawa — 1
Department of Meteorology
University of California
Los Angeles, California 90024

12. Atmospheric Sciences Library — 1
National Oceanic and Atmospheric Administration
Silver Spring, Maryland 20910

13. Dr. John Brown — 1
National Meteorological Center/NOAA
World Weather Building
Washington, D.C. 20233

14. Dr. C.-P. Chang, Code 63Cj — 1
Department of Meteorology
Naval Postgraduate School
Monterey, California 93940

15. Dr. R. L. Elsberry, Code 63Es — 1
Department of Meteorology
Naval Postgraduate School
Monterey, California 93940

16. Dr. G. J. Haltiner, Code 63Ha — 1
Chairman, Department of Meteorology
Naval Postgraduate School
Monterey, California 93940

17. Dr. R. L. Haney, Code 63Hy — 1
Department of Meteorology
Naval Postgraduate School
Monterey, California 93940

18. Dr. J. Holton — 1
Department of Atmospheric Sciences
University of Washington
Seattle, Washington 98105

19. Dr. A. Kasahara — 1
National Center for Atmospheric Research
P. O. Box 3000
Boulder, Colorado 80303

20. Dr. J. D. Mahlman — 1
Geophysical Fluid Dynamics Laboratory
Princeton University
Princeton, New Jersey 08540

21. Meteorology Library (Code 63) — 1
Naval Postgraduate School
Monterey, California 93940

22. National Center for Atmospheric Research — 1
Box 1470
Boulder, Colorado 80302

23. Office of Naval Research — 1
Department of the Navy
Washington, D. C. 20360

24. Professor N. A. Phillips — 1
National Meteorological Center/NOAA
World Weather Building
Washington, D. C. 20233

25. Dr. S. Piacsek — 1
Code 7750
Naval Research Laboratory
Washington, D. C. 20390

26. Dr. Y. Sasaki — 1
Environmental Prediction Research Facility
Naval Postgraduate School
Monterey, California 93940

27. Dr. J. Smagorinsky, Director — 1
Geophysical Fluid Dynamics Laboratory
Princeton University
Princeton, New Jersey 08540

28. Dr. D. Williamson — 1
National Center for Atmospheric Research
P. O. Box 3000
Boulder, Colorado 80303

29. Dr. T. Rosmond — 1
Naval Environmental Prediction Research Facility
Monterey, California 93940

30. Lieutenant W. F. Mihok — 1
Fleet Numerical Weather Central
Monterey, California 93940

31. Dr. D. Dietrick — 1
JAYCOR
205 S. Whiting Street, Suite 409
Alexandria, Virginia 22304